Available online at www.sciencedirect.com

ScienceDirect

Procedia Computer Science 4 (2011) 948–957

Procedia Computer Science

ICCS 2011

A Finite Difference Scheme for Double-Diffusive Unsteady Free Convection from a Curved Surface to a Saturated Porous Medium with a Non-Newtonian Fluid

M. F. El-Amin[a,b,*], Shuyu Sun[a]

[a]*King Abdullah University of Science and Technology (KAUST), Thuwal 23955-6900, KSA*
[b]*Aswan Faculty of Science, South Valley University, Aswan 81528, Egypt*

Abstract

In this paper, a finite difference scheme is developed to solve the unsteady problem of combined heat and mass transfer from an isothermal curved surface to a porous medium saturated by a non-Newtonian fluid. The curved surface is kept at constant temperature and the power-law model is used to model the non-Newtonian fluid. The explicit finite difference method is used to solve simultaneously the equations of momentum, energy and concentration. The consistency of the explicit scheme is examined and the stability conditions are determined for each equation. Boundary layer and Boussinesq approximations have been incorporated. Numerical calculations are carried out for the various parameters entering into the problem. Velocity, temperature and concentration profiles are shown graphically. It is found that as time approaches infinity, the values of wall shear, heat transfer coefficient and concentration gradient at the wall, which are entered in tables, approach the steady state values.

Keywords: Finite difference method; stability; power-law fluids; porous medium; mass transfer; free convection

1. Introduction

The study of physics of the flow through porous media has many applications, such as geothermal fields, soil pollution, fibrous insulation and nuclear-waste disposal. Also, a number of industrially important fluids such as molten plastics, polymers, pulps, foods and slurries display non-Newtonian fluid behavior. Non-Newtonian fluids exhibit a non-linear relationship between shear stress and shear rate. Chen and Chen [1] presented similarity solutions for free convection of non-Newtonian fluids over vertical surfaces in porous media. The problem of buoyancy induced flow of non-Newtonian fluids over a non-isothermal horizontal plate embedded in a porous medium was studied by Mehta and Rao [2] by introducing a general similarity transformation procedure. Darcy-Forchheimer natural, forced and mixed convection heat transfer in power-law fluid saturated porous media was

* Corresponding author. Tel.: +966-59-737-5091.
E-mail address: mohamed.elamin@kaust.edu.sa.

Selection and/or peer-review under responsibility of Prof. Mitsuhisa Sato and Prof. Satoshi Matsuoka
doi:10.1016/j.procs.2011.04.100

studied by Shenoy [3]. Nakayama and Koyama [4] studied the natural convection over a non-isothermal body of arbitrary shape embedded in a porous medium. All these studies were concerned with steady flows. Unsteady natural heat transfer from a curved surface to a non-Newtonian pseudoplastic liquid is investigated by Roy [5]. Haq and Mulligan [6] studied the problem of transient free convection from a vertical plate to a non-Newtonian fluid in a porous medium. Unsteady free convection flow of a non-Newtonian fluid through a porous medium bounded by a vertical surface was investigated by Hady et al. [7]. Natural convection flows due to combined buoyancy effects of thermal and species diffusion in a fluid saturated porous medium have many applications. Unsteady free convective flow and mass transfer through a porous medium bounded by an infinite vertical limiting surface with constant suction and time-dependent temperature studied by Raptis [8]. Kumari and Nath [9] studied the unsteady laminar natural convection of an electrically conducting fluid over two-dimensional and axisymmetric bodies in a porous medium with an applied magnetic field. Unsteady mixed convection adjacent to a vertical surface with combined buoyancies in the presence of magnetic field was numerically studied by the same authors [10]. Unsteady magneto-hydrodynamic mixed convection with combined buoyancies over a horizontal cylinder and a sphere was also reported [11]. Pop and Herwing [12] studied the transient development of the concentration boundary layer with impulsive mass diffusion from a heated vertical surface. The problem of unsteady free convection adjacent to an impulsively heated horizontal circular cylinder in porous media was investigated by Bradean et al. [13]. Numerical study of double-diffusive free convection from a vertical surface is presented by Srinivasan and Angirasa [14]. More recently, Angirasa et al. [15] investigated combined heat and mass transfer by natural convection with opposing buoyancy effects in a fluid saturated porous medium. Rastogi and Poulikakos [16] considered non-Newtonian fluid saturated porous media and presented similarity solutions for aiding flows with concentration. The problem of forced convection heat transfer on a flat plate embedded in porous media for power-law fluids has been studied by Hady and Ibrahim [17].

The purpose of this paper is to study the problem of unsteady combined heat and mass transfer by natural convection from an isothermal curved surface which is kept at constant temperature to a non-Newtonian power-law fluid saturated porous medium. The dimensionless non-linear partial differential equations are solved numerically using an explicit finite-difference scheme. The values of wall shear, heat transfer coefficient and concentration gradient at the wall are determined for steady and unsteady free convection.

2. Mathematical Formulation

The physical configuration and the coordinate system used in the current investigation are shown in Fig. 1. An isothermal curved surface at constant temperature is embedded in a non-Newtonian power-law fluid saturated porous medium. In this study, in accordance with previous work reported by Shulman et al. [18] and Shvets and Vishnevskeiy [19] the following transport properties based on the power-law model are assumed to hold.

$$\tau_{ij} = -p\delta_{ij} + k\left|\frac{1}{2}I_2\right|^{(n-1)/2} e_{ij} \tag{1}$$

where τ_{ij} and e_{ij} are the tensors of stress and strain rate, k is the non-Newtonian consistency index, δ_{ij} is the unit tensor, I_2 is the second invariant of the strain rate, p is the pressure and n is the power flow behavior index of the fluid (n>0). For n=1, it reduces to a Newtonian fluid, for values of n<1 the behavior is pseudoplastic and, when n>1, the fluid is dilatant.

Under the Boussinesq, boundary layer and dilute solution approximations, the governing mass, momentum, energy and species conservation equations for free convective flows driven by temperature and concentration differences become,

$$\frac{\partial \bar{u}}{\partial \bar{x}} + \frac{\partial \bar{v}}{\partial \bar{y}} = 0 \tag{2}$$

$$\frac{\partial \bar{u}}{\partial \bar{t}} + \bar{u}\frac{\partial \bar{u}}{\partial \bar{x}} + \bar{v}\frac{\partial \bar{u}}{\partial \bar{y}} = g[\beta(\bar{T} - \bar{T}_\infty) + \beta^*(\bar{C} - \bar{C}_\infty)]\sin\omega + \frac{k}{\rho}\frac{\partial}{\partial \bar{y}}\left(\left|\frac{\partial \bar{u}}{\partial \bar{y}}\right|^{n-1}\frac{\partial \bar{u}}{\partial \bar{y}}\right) - \frac{k\varepsilon^n}{\rho \mathrm{K}}|\bar{u}|^{n-1}\bar{u} - \frac{F\varepsilon^2}{\mathrm{K}^{1/2}}|\bar{u}|\bar{u} \tag{3}$$

$$\frac{\partial \overline{T}}{\partial \overline{t}} + \overline{u}\frac{\partial \overline{T}}{\partial \overline{x}} + \overline{v}\frac{\partial \overline{T}}{\partial \overline{y}} = \alpha \frac{\partial^2 \overline{T}}{\partial \overline{y}^2} \tag{4}$$

$$\frac{\partial \overline{C}}{\partial \overline{t}} + \overline{u}\frac{\partial \overline{C}}{\partial \overline{x}} + \overline{v}\frac{\partial \overline{C}}{\partial \overline{y}} = D\frac{\partial^2 \overline{C}}{\partial \overline{y}^2} \tag{5}$$

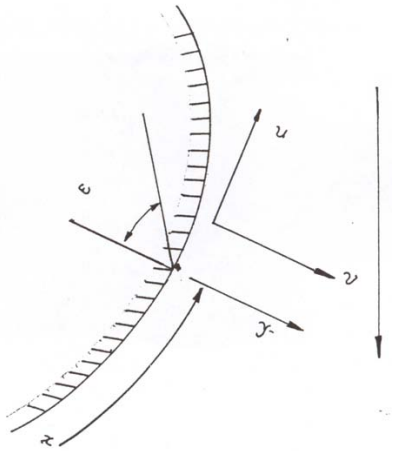

Fig. 1 Flow model and coordinate system

In these equations, $\overline{u}$ and $\overline{v}$ are the velocity components along $\overline{x}$ and $\overline{y}$ axes. The temperature of the surface is $\overline{T}_w$ and the surface concentration of the diffusing species is $\overline{C}_w$. Far away from the surface these values are invariant and are represented by $\overline{T}$ and $\overline{C}$, respectively. $\rho, \alpha, D, \beta, \beta^*, \varepsilon, F, K, \omega$ and g are the density, the thermal diffusivity, the species diffusion coefficient, the volumetric coefficient of thermal expansion, the volumetric coefficient expansion with concentration, the porosity, the empirical constant, the permeability, angle is shown in Fig. 1 and acceleration due to gravity, respectively. The boundary and initial conditions are,

$$\overline{t} = 0: \ \overline{u} = \overline{v} = 0, \ \overline{T} = \overline{T}_\infty, \overline{C} = \overline{C}_\infty \quad \text{for all } \overline{x} \text{ and } \overline{y}$$

$$\overline{t} > 0: \begin{cases} \overline{u} = \overline{v} = 0, \ \overline{T} = \overline{T}_\infty, \overline{C} = \overline{C}_\infty & \text{at } \overline{x} = 0 \\ \overline{u} = \overline{v} = 0, \overline{T} = \overline{T}_w, \overline{C} = \overline{C}_w & \text{at } \overline{y} = 0, \overline{x} > 0 \\ \overline{u} = 0, \overline{T} = \overline{T}_\infty, \overline{C} = \overline{C}_\infty & \text{at } \overline{y} \to \infty, \overline{x} > 0 \end{cases} \tag{6}$$

At time $\overline{t} = 0$, the temperature of the surface immersed in a fluid is raised suddenly from that of surrounding fluid $\overline{T}_\infty$, up to a higher and constant value $\overline{T}_w$ and kept at this value thereafter.

We introduce the following dimensionless variables,

$$x = \frac{\overline{x}}{L}, \ y = \frac{\overline{y}}{L}, \ u = \frac{\overline{u}}{U}, \ v = \frac{\overline{v}}{U}, \ T = \frac{\overline{T} - \overline{T}_\infty}{\overline{T}_w - \overline{T}_\infty}, \ C = \frac{\overline{C} - \overline{C}_\infty}{\overline{C}_w - \overline{C}_\infty} \text{ and } t = \frac{U\overline{t}}{L} \tag{7}$$

where $U = [\rho L^n / k]^{1/n-2}$ and L is a suitable length scale.

Introducing expressions (7) into equations (2)-(5), we have,

$$\frac{\partial u}{\partial x} + \frac{\partial v}{\partial y} = 0 \tag{8}$$

$$\frac{\partial u}{\partial t} + u\frac{\partial u}{\partial x} + v\frac{\partial u}{\partial y} = GrT + GmC + \frac{\partial}{\partial y}\left(\left|\frac{\partial u}{\partial y}\right|^{n-1}\frac{\partial u}{\partial y}\right) - k_1|u|^{n-1}u - k_2|u|u \tag{9}$$

$$\frac{\partial T}{\partial t}+u\frac{\partial T}{\partial x}+v\frac{\partial T}{\partial y}=\frac{1}{\mathrm{Re}\,\mathrm{Pr}}\frac{\partial^2 T}{\partial y^2} \tag{10}$$

$$\frac{\partial C}{\partial t}+u\frac{\partial C}{\partial x}+v\frac{\partial C}{\partial y}=\frac{1}{\mathrm{Re}\,Sc}\frac{\partial^2 C}{\partial y^2} \tag{11}$$

where $Gr = Lg\beta(\overline{T}_w-\overline{T}_\infty)\sin\omega/U^2$ is the Grashof number, $Gm = Lg\beta^*(\overline{C}_w-\overline{C}_\infty)\sin\omega/U^2$ is the modified Grashof number, $k_1=\varepsilon^n L^{n+1}/K$ and $k_2=F\varepsilon^2 L/K^{1/2}$ are the dimensionless first and second-order resistances due to the presence of the solid matrix, $\mathrm{Re}=\rho LU/k$ is the Reynolds number, $\mathrm{Pr}=k/\rho\alpha$ is the Prandtl number and $Sc=k/\rho D$ is the Schmidt number.

The boundary and initial conditions are now given by,

$$t=0:\ u=v=T=C=0 \quad \text{for all } x \text{ and } y$$

$$t>0:\begin{cases} u=v=T=C=0 & \text{at } x=0 \\ u=v=0,\ T=1,\ C=1 & \text{at } y=0,\ x>0 \\ u=0,\ T=0,\ C=0 & \text{at } y\to\infty,\ x>0 \end{cases} \tag{12}$$

In technological applications, the wall shear stress, the local Nusselt number and the Sherwood number are of primary interest.

The wall shear stress may be written as,

$$\tau_w=k\left(\frac{\partial\overline{u}}{\partial\overline{y}}\right)^n\Bigg|_{\overline{y}=0}=k\frac{U^n}{L^n}\left(\frac{\partial u}{\partial y}\right)^n\Bigg|_{y=0} \tag{13}$$

Therefore the local friction factor is given by,

$$C_f=\frac{2\tau_w}{\rho U^2}=2\left(\frac{\partial u}{\partial y}\right)^n\Bigg|_{y=0} \tag{14}$$

From the definition of the local surface heat flux is defined by,

$$q_w=-k_e\frac{\partial\overline{T}}{\partial\overline{y}}\Bigg|_{\overline{y}=0}=-\frac{k_e(\overline{T}_w-\overline{T}_\infty)}{L}\frac{\partial T}{\partial y}\Bigg|_{y=0} \tag{15}$$

where k_e is the effective thermal conductivity of the saturated porous medium, together with the definition of the local Nusselt number,

$$Nu=\frac{q_w}{\overline{T}_w-\overline{T}_\infty}\frac{L}{k_e}=-\frac{\partial T}{\partial y}\Bigg|_{y=0} \tag{16}$$

The local mass flux is given by,

$$j_w=-D\frac{\partial\overline{C}}{\partial\overline{y}}\Bigg|_{\overline{y}=0} \tag{17}$$

Therefore, Sherwood number is defined by,

$$Sh=\frac{j_w L}{D(\overline{C}_w-\overline{C}_\infty)}=-\frac{\partial C}{\partial y}\Bigg|_{y=0} \tag{18}$$

3. An Explicit Finite Difference Scheme

The solution of a set of simultaneous nonlinear partial differential equations by the explicit finite-difference method was given by Carnahan et al. [20]. The system of nonlinear partial differential equations (8)-(11), with initial and boundary conditions (12), were solved for the dependent variables *u*, *v*, *T* and *C* as functions of *x*, *y* and *t*. The steady state condition was assumed to exist when $\partial u/\partial t$, $\partial T/\partial t$ and $\partial C/\partial t$ approached zero in the unsteady state problem, formulated in the previous section. Successive steps in time can then be regarded as successive

approximations toward the steady state solution. The spatial domain under investigation was restricted to finite dimensions. Here, the length of the plate X_{max} was assumed to be 50 and the boundary layer thickness Y_{max} was taken as 20.

Consider u', v' , T' and C' denote the values of u, v, T and C at the end of a time-step. Then, the approximate set of finite difference equations corresponding to the system of (8)-(11) are,

$$\frac{u'_{i,j}-u'_{i-1,j}}{\Delta x}+\frac{v'_{i,j}-v'_{i,j-1}}{\Delta y}=0 \tag{19}$$

$$\frac{u'_{i,j}-u_{i,j}}{\Delta t}+u_{i,j}\frac{u_{i,j}-u_{i-1,j}}{\Delta x}+v_{i,j}\frac{u_{i,j+1}-u_{i,j}}{\Delta y}=GrT'+GmC'+$$
$$\left\{\left|\frac{u_{i,j+1}-u_{i,j}}{\Delta y}\right|^{n-1}\left(\frac{u_{i,j+1}-u_{i,j}}{\Delta y}\right)-\left|\frac{u_{i,j}-u_{i,j-1}}{\Delta y}\right|^{n-1}\left(\frac{u_{i,j}-u_{i,j-1}}{\Delta y}\right)\right\}\Big/\Delta y \tag{20}$$
$$-k_1\left|u_{i,j}\right|^{n-1}u_{i,j}-k_2\left|u_{i,j}\right|u_{i,j}$$

$$\frac{T'_{i,j}-T_{i,j}}{\Delta t}+u_{i,j}\frac{T_{i,j}-T_{i-1,j}}{\Delta x}+v_{i,j}\frac{T_{i,j+1}-T_{i,j}}{\Delta y}=\frac{1}{\mathrm{Re}\,\mathrm{Pr}}\left(\frac{T_{i,j+1}-2T_{i,j}+T_{i,j-1}}{(\Delta y)^2}\right) \tag{21}$$

$$\frac{C'_{i,j}-C_{i,j}}{\Delta t}+u_{i,j}\frac{C_{i,j}-C_{i-1,j}}{\Delta x}+v_{i,j}\frac{C_{i,j+1}-C_{i,j}}{\Delta y}=\frac{1}{\mathrm{Re}\,Sc}\left(\frac{C_{i,j+1}-2C_{i,j}+C_{i,j-1}}{(\Delta y)^2}\right) \tag{22}$$

where primed variables indicate the values of the variables at a new time and (*i, j*) represent grid points.

The coefficients $u_{i,j}$,$v_{i,j}$, $\left|(u_{i,j+1}-u_{i,j})/\Delta y\right|^{n-1}$ and $\left|(u_{i,j}-u_{i,j-1})/\Delta y\right|^{n-1}$ in Eq. (20) are treated as constants, during any one time-step, for the values of n, $0.5\le n\le 2$. Then, at the end of any time-step Δt, the new velocity components u' and v', the new temperature T' and the new concentration C' at all interior grid points may be obtained by successive applications of (21), (22), (20) and (19), respectively. This process is repeated in time and provided the time-step is sufficiently small, u, v, T and C should eventually converge to values, which approximate the steady state solution of Eqs. (19)-(22).

The velocity, temperature fields and concentration distributions were calculated for various time steps for a 100×60 grid. A comprehensive set of results have been obtained covering the ranges $0.5\le n\le 2.0$, $1\le \mathrm{Re}\,\mathrm{Pr}\le 10$, $0.5\le \mathrm{Re}\,Sc\le 10$, $0.0\le Gr\le 1.0$, $0.0\le Gm\le 1.0$, $0.05\le k_1\le 0.5$, and $0.05\le k_2\le 0.5$. A selection of these results is presented here with a view to isolate the effect of each individual parameter. An examination of complete results for t=10, 20,..., 70, revealed little or no change in u, v, T and C after t=70 for all computations. Thus the results for t=70 are essentially the steady-state values.

4. Consistency of the Scheme

When, the finite difference procedure approximate the solution of the partial differential equation under study and not the solution of any other partial differential equation, then, the procedure is called have consistency. The consistency is measured in terms of the difference between a differential equation and difference equation.

$$\frac{\partial u}{\partial t}=\frac{u'_{i,j}-u_{i,j}}{\Delta t}+O(\Delta t),\ \frac{\partial u}{\partial x}=\frac{u_{i,j}-u_{i-1,j}}{\Delta x}+O(\Delta x),\ \frac{\partial u}{\partial y}=\frac{u_{i,j+1}-u_{i,j}}{\Delta y}+O(\Delta y),$$

$$\frac{\partial^2 u}{\partial y^2}=\frac{u_{i,j+1}-2u_{i,j}+u_{i,j-1}}{(\Delta y)^2}+O(\Delta y)^2,\ \frac{\partial T}{\partial t}=\frac{T'_{i,j}-T_{i,j}}{\Delta t}+O(\Delta t),$$

$$\frac{\partial T}{\partial x}=\frac{T_{i,j}-T_{i-1,j}}{\Delta x}+O(\Delta x),\ \frac{\partial T}{\partial y}=\frac{T_{i,j+1}-T_{i,j}}{\Delta y}+O(\Delta y),\ \frac{\partial^2 T}{\partial y^2}=\frac{T_{i,j+1}-2T_{i,j}+T_{i,j-1}}{(\Delta y)^2}+O(\Delta y)^2,$$

$$\frac{\partial \mathrm{C}}{\partial t}=\frac{C'_{i,j}-C_{i,j}}{\Delta t}+O(\Delta t),\ \frac{\partial C}{\partial x}=\frac{C_{i,j}-C_{i-1,j}}{\Delta x}+O(\Delta x),\ \frac{\partial C}{\partial y}=\frac{C_{i,j+1}-C_{i,j}}{\Delta y}+O(\Delta y),$$

$$\frac{\partial^2 C}{\partial y^2}=\frac{C_{i,j+1}-2C_{i,j}+C_{i,j-1}}{(\Delta y)^2}+O(\Delta y)^2$$

In order to examine the consistency of equations (20) and (22), substituting the above expressions into equation (20) and (22), we have

$$\left[\frac{u'_{i,j}-u_{i,j}}{\Delta t}+u_{i,j}\frac{u_{i,j}-u_{i-1,j}}{\Delta x}+v_{i,j}\frac{u_{i,j+1}-u_{i,j}}{\Delta y}-GrT'_{i,j}-GmC'_{i,j}-\right.$$
$$\left.\left\{\left|\frac{u_{i,j+1}-u_{i,j}}{\Delta y}\right|^{n-1}\left(\frac{u_{i,j+1}-u_{i,j}}{\Delta y}\right)-\left|\frac{u_{i,j}-u_{i,j-1}}{\Delta y}\right|^{n-1}\left(\frac{u_{i,j}-u_{i,j-1}}{\Delta y}\right)\right\}\Big/\Delta y+\right. \tag{23}$$
$$\left.k_1\left|u_{i,j}\right|^{n-1}u_{i,j}+k_2\left|u_{i,j}\right|u_{i,j}\right]-\left[\frac{\partial u}{\partial t}+u\frac{\partial u}{\partial x}+v\frac{\partial u}{\partial y}-\frac{\partial}{\partial y}\left(\left|\frac{\partial u}{\partial y}\right|^{n-1}\frac{\partial u}{\partial y}\right)\right]_{i,j}$$
$$=O(\Delta t)+u_{i,j}O(\Delta x)+v_{i,j}O(\Delta y)+O(\Delta y)^{n+1}$$

$$\left[\frac{T'_{i,j}-T_{i,j}}{\Delta t}+u_{i,j}\frac{T_{i,j}-T_{i-1,j}}{\Delta x}+v_{i,j}\frac{T_{i,j+1}-T_{i,j}}{\Delta y}-\right.$$
$$\left.\frac{1}{\mathrm{Pr}}\left(\frac{T_{i,j+1}-2T_{i,j}+T_{i,j-1}}{(\Delta y)^2}\right)-\left[\frac{\partial T}{\partial t}+u\frac{\partial T}{\partial x}+v\frac{\partial T}{\partial y}-\frac{1}{\mathrm{Pr}}\frac{\partial^2 T}{\partial y^2}\right]_{i,j}\right. \tag{24}$$
$$=O(\Delta t)+u_{i,j}O(\Delta x)+v_{i,j}O(\Delta y)+\frac{1}{\mathrm{Re}\,\mathrm{Pr}}O(\Delta y)^2$$

$$\left[\frac{C'_{i,j}-C_{i,j}}{\Delta t}+u_{i,j}\frac{C_{i,j}-C_{i-1,j}}{\Delta x}+v_{i,j}\frac{C_{i,j+1}-C_{i,j}}{\Delta y}-\right.$$
$$\left.\frac{1}{Sc}\left(\frac{C_{i,j+1}-2C_{i,j}+C_{i,j-1}}{(\Delta y)^2}\right)-\left[\frac{\partial \mathrm{C}}{\partial t}+u\frac{\partial \mathrm{C}}{\partial x}+v\frac{\partial \mathrm{C}}{\partial y}-\frac{1}{Sc}\frac{\partial^2 C}{\partial y^2}\right]_{i,j}\right. \tag{25}$$
$$=O(\Delta t)+u_{i,j}O(\Delta x)+v_{i,j}O(\Delta y)+\frac{1}{\mathrm{Re}\,Sc}O(\Delta y)^2$$

From equations (23)-(25) we note that, the R.H.S. represents the truncation error which is tends to zero as $\Delta t, \Delta x, \Delta y \to 0$. Therefore, the explicit scheme is consistent.

5. Stability Conditions of the Scheme

Here, the stability conditions of the finite difference scheme are determined. As an explicit procedure is used we intent to investigate the largest time-step consistent with the stability. Because, *t* does not appear in the continuity equation, it will be ignored. At an arbitrary time $t=1$, the general terms of the Fourier expansion for *u*, *T* and *C* are become $e^{i'(ax+by)}$, $i'=\sqrt{-1}$. At a later time *t*, these terms will become $u=\psi(t)e^{i'(ax+by)}$, $T=\zeta(t)e^{i'(ax+by)}$, $C=\phi(t)e^{i'(ax+by)}$.

Substituting in (20)-(22) and regarding the coefficients *u* and *v* as constants over any one time-step and denoting the values of ψ, ζ and ϕ after the time-step by ψ', ζ' and ϕ', we obtain,

$$\frac{\psi'-\psi}{\Delta t}+u\frac{\psi(1-e^{-i'a\Delta x})}{\Delta x}+v\frac{\psi(e^{i'b\Delta y}-1)}{\Delta y}=Gr\zeta'+Gm\phi'+\psi\left\{\left|\frac{u_{i,j+1}-u_{i,j}}{\Delta y}\right|^{n-1}\left(\frac{(e^{i'b\Delta y}-1)}{\Delta y}\right)-\left|\frac{u_{i,j}-u_{i,j-1}}{\Delta y}\right|^{n-1}\left(\frac{(1-e^{-i'b\Delta y})}{\Delta y}\right)\right\}\Big/\Delta y-k_1|u|^{n-1}\psi-k_2|u|\psi \tag{26}$$

$$\frac{\zeta'-\zeta}{\Delta t}+u\frac{\zeta(1-e^{-i'a\Delta x})}{\Delta x}+v\frac{\zeta(e^{i'b\Delta y}-1)}{\Delta y}=\frac{2}{\mathrm{Re}\,\mathrm{Pr}(\Delta y)^2}(\cos b\Delta y-1)\zeta \tag{27}$$

$$\frac{\phi'-\phi}{\Delta t}+u\frac{\phi(1-e^{-i'a\Delta x})}{\Delta x}+v\frac{\phi(e^{i'b\Delta y}-1)}{\Delta y}=\frac{2}{\mathrm{Re}\,Sc(\Delta y)^2}(\cos b\Delta y-1)\phi \tag{28}$$

We note that the coefficients $\left|(u_{i,j+1}-u_{i,j})/\Delta y\right|^{n-1}$, $\left|(u_{i,j}-u_{i,j-1})/\Delta y\right|^{n-1}$ are very close to unity, because, the choice the exponent lie in the interval. We assume that

$$A=1-\frac{u\Delta t}{\Delta x}(1-e^{-i'a\Delta x})-\frac{v\Delta t}{\Delta y}(e^{i'b\Delta y}-1)+\frac{\Delta t}{(\Delta y)^2}\left\{\left|\frac{u_{i,j+1}-u_{i,j}}{\Delta y}\right|^{n-1}(e^{i'b\Delta y}-1)-\left|\frac{u_{i,j}-u_{i,j-1}}{\Delta y}\right|^{n-1}(1-e^{-i'b\Delta y})\right\}-k_1|u|^{n-1}-k_2|u| \tag{29}$$

$$B=1-\frac{u\Delta t}{\Delta x}(1-e^{-i'a\Delta x})-\frac{v\Delta t}{\Delta y}(e^{i'b\Delta y}-1)+\frac{2\Delta t}{\mathrm{Re}\,\mathrm{Pr}(\Delta y)^2}(\cos b\Delta y-1) \tag{30}$$

$$E=1-\frac{u\Delta t}{\Delta x}(1-e^{-i'a\Delta x})-\frac{v\Delta t}{\Delta y}(e^{i'b\Delta y}-1)+\frac{2\Delta t}{\mathrm{Re}\,Sc(\Delta y)^2}(\cos b\Delta y-1) \tag{31}$$

Using equations (26)-(31), one can write

$$\begin{bmatrix}\psi'\\ \zeta'\\ \phi'\end{bmatrix}=\begin{bmatrix}A & GrB\Delta t & GmE\Delta t\\ 0 & B & 0\\ 0 & 0 & E\end{bmatrix}\begin{bmatrix}\psi\\ \zeta\\ \phi\end{bmatrix}$$

In order to seek the stability of the previous system, the moduli of each of the eigenvalues λ_1, λ_2 and λ_3 of the coefficients matrix should be less than or equal to unity. Here, we have $\lambda_1=A$, $\lambda_2=B$ and $\lambda_3=E$. Therefore, the stability conditions are $|A|\le 1$, $|B|\le 1$ and $|E|\le 1$, for all *a* and *b*.

Since, the heated fluid rises in the positive *x*-direction, *u* may be assumed everywhere non-negative. Also, we assume that *v* to be everywhere non-positive, because, the fluid is drawn in from the positive *y*-direction to take its place. We can assume, at any case, that,

$\alpha=\frac{u\Delta t}{\Delta x}$, $\beta=\frac{|v|\Delta t}{\Delta y}$, $\gamma=\frac{\Delta t}{(\Delta y)^2}$, $\delta=\frac{u\Delta t}{(\Delta y)^2}$, $c_1=\left|(u_{i,j+1}-u_{i,j})/\Delta y\right|^{n-1}$, $c_2=\left|(u_{i,j}-u_{i,j-1})/\Delta y\right|^{n-1}$, $c_3=k_1|u|^{n-1}$ and $c_4=k_2|u|$

Therefore,

$$A=1-\alpha(1-e^{-i'a\Delta x})-\beta(e^{i'b\Delta y}-1)+\gamma\left\{c_1(e^{i'b\Delta y}-1)-c_2(1-e^{-i'b\Delta y})\right\}-c_3-c_4$$

$$B=1-\alpha(1-e^{-i'a\Delta x})-\beta(e^{i'b\Delta y}-1)+2\frac{\gamma}{\mathrm{Re}\,\mathrm{Pr}}(\cos b\Delta y-1)$$

$$E=1-\alpha(1-e^{-i'a\Delta x})-\beta(e^{i'b\Delta y}-1)+2\frac{\gamma}{\mathrm{Re}\,Sc}(\cos b\Delta y-1)$$

The coefficients α,β,γ and δ are positive and real. Representing *A*, *B* and *E* on an Argand diagram, the maximum values of $|A|$, $|B|$ and $|E|$ occur when $a\Delta x=r\pi$ and $b\Delta y=s\pi$, where *r* and *s* are positive integers. The values of $|A|$, $|B|$ and $|E|$ are maximum, for Δt sufficiently large, when both *r* and *s* are odd integers. In this case we have

$A = 1 - 2[\alpha + \beta + \gamma(c_1 + c_2)] - c_3 - c_4$, $B = 1 - 2[\alpha + \beta + 2\frac{\gamma}{\mathrm{Re}\,\mathrm{Pr}}]$, $E = 1 - 2[\alpha + \beta + 2\frac{\gamma}{\mathrm{Re}\,Sc}]$

To satisfy $|A| \le 1$, $|B| \le 1$ and $|E| \le 1$ the most negative allowable value is $A=B=E=-1$, then, the stability conditions can be written as

$$\alpha + \beta + \gamma(c_1 + c_2) + \frac{c_3 + c_4}{2} \le 1 \quad (32)$$

$$\alpha + \beta + 2\frac{\gamma}{\mathrm{Re}\,\mathrm{Pr}} \le 1 \quad (33)$$

$$\alpha + \beta + 2\frac{\gamma}{\mathrm{Re}\,Sc} \le 1 \quad (34)$$

In order to satisfy the first stability condition (32), we choice $0.03 \le k_1 \le 0.05$ and $0.02 \le k_2 \le 0.04$, which make values of c_3 and c_4 smaller, with noting that c_1 and c_2 close to unity as explained above. Also, the choice $1 \le \mathrm{Re}\,\mathrm{Pr} \le 10$ satisfies the second stability condition (33), and the choice $0.5 \le \mathrm{Re}\,Sc \le 10$ satisfies the third stability condition (34).

6. Results and Discussion

The numerical scheme used the finite difference method to solve the system of non-linear partial differential equations (8)-(11) subject to the initial and boundary conditions (12).

Table 1. $C_f/2$, *Nu* and *Sh* for various values of *n* for *Gr*=0.5, *Gm*=0.5, *RePr*=5.0, *ReSc*=0.5, k_1=0.05 and k_2=0.05 at *X*=20

T	*n*	$C_f/2$	*Nu*	*Sh*
20	0.5	0.831072	0.281989	0.101457
	1.0	0.805525	0.285517	0.100398
	1.5	0.736557	0.286553	0.100356
	2.0	0.670711	0.286380	0.099575
40	0.5	0.821778	0.284557	0.104757
	1.0	0.805112	0.288100	0.100942
	1.5	0.736526	0.287805	0.100373
	2.0	0.670579	0.287041	0.099213
60	0.5	0.821760	0.284579	0.104758
	1.0	0.805040	0.288121	0.100986
	1.5	0.736428	0.287819	0.100454
	2.0	0.670497	0.287000	0.099311
80	0.5	0.821760	0.284579	0.104758
	1.0	0.805040	0.288121	0.100986
	1.5	0.736428	0.287819	0.100454
	2.0	0.670496	0.287001	0.099311
∞	0.5	0.821760	0.284579	0.104758
	1.0	0.805040	0.288121	0.100986
	1.5	0.736428	0.287819	0.100454
	2.0	0.670496	0.287001	0.099311

Table 2. $C_f/2$, *Nu* and *Sh* for various values of *n*, k_1 and k_2 for *Gr*=*Gm*=0.5, *RePr*=5.0, *ReSc*=0.5, at *X*=20

n	k_1	k_2	$C_f/2$	*Nu*	*Sh*
0.5	0.05	0.05	0.821760	0.284579	0.104758
		0.1	0.770325	0.271916	0.097815
		0.5	0.595192	0.229156	0.078330
	0.1	0.05	0.778273	0.272806	0.097561
		0.1	0.737164	0.262850	0.092538
		0.5	0.582689	0.225888	0.076991
1.0	0.05	0.05	0.805040	0.288121	0.100986
		0.1	0.713676	0.274377	0.093661
		0.5	0.457948	0.225429	0.072504
	0.1	0.05	0.736538	0.278319	0.095111
		0.1	0.663605	0.266417	0.089118
		0.5	0.441426	0.221674	0.070503
1.5	0.1	0.05	0.647154	0.277995	0.094448
		0.1	0.568764	0.268073	0.089082
		0.5	0.323136	0.226151	0.071125

Tabs. 1-4 represent the variation of the friction factor, Nusselt number and Sherwood number for pseudoplastic fluid, Newtonian fluid and dilatant fluid for various values of the parameters *t, k_1, k_2, RePr, ReSc*, *Gr* and *Gm*.

Table 3. $C_f/2$, *Nu* and *Sh* for various values of RePr and ReSc when k1=k2=0.05, Gr=Gm=0.5 and n=1.5 at X=20.

RePr	ReSc	$C_f/2$	Nu	Sh
5.0	0.5	0.736429	0.287819	0.100454
	1.0	0.689189	0.282613	0.136017
	5.0	0.538846	0.262875	0.262875
10.0	0.5	0.671398	0.351867	0.098544
	1.0	0.623278	0.347058	0.132485
	5.0	0.474263	0.327979	0.253237

Table 4. $C_f/2$, *Nu* and *Sh* for various values of *Gr*, *Gm* at *RePr*=5.0, *ReSc*=0.5, k_1=k_2=0.05, n=0.5 at X=20.

Gr	Gm	$C_f/2$	Nu	Sh
1.0	1.0	1.054089	0.328269	0.154343
	0.5	0.908943	0.299188	0.107085
	0.0	0.699568	0.240289	0.077589
0.5	1.0	0.951849	0.319907	0.145859
	0.5	0.821760	0.284579	0.104758
	0.0	0.538991	0.196197	0.067199

Numerical results of transient friction factor, Nusselt number and Sherwood number for different values of the power-law index n are presented in Tab. 1. From this table we note that both the wall shear stress and the mass transfer rate is reduced with n, while they are enhanced with time. Also, it can be seen that, the heat transfer rate increases with n and t when $n \le 1$, and the opposite is true when $n \ge 1$. Tab. 2 indicates that, an increase in the values of the parameters k_1 and k_2 reduces the wall shear stress, the heat transfer rate and the concentration gradient at the wall. From Tab. 3 it can be seen that due to an increase in *RePr* there is a fall in the wall shear stress and the concentration gradient at the wall, but, there is an increase in the heat transfer rate. Also, from the same table we note that as *ReSc* increases both the wall shear stress and the heat transfer rate decreases, while, the concentration gradient at the wall increases. It is obvious that, an increase in the values of the parameters *Gr* and *Gm* enhances the wall shear stress, the heat transfer rate and the concentration gradient at the wall, as shown in Tab. 4.

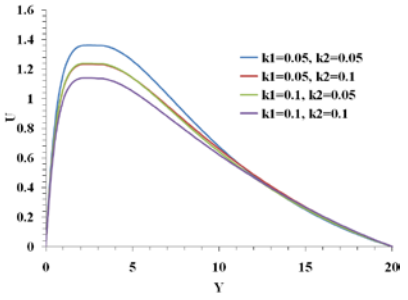

Fig. 2. Steady state velocity profiles for various values of k_1 and k_2 when n=0.5, *Gr*=*Gm*=0.5, *RePr*=5.0 and *ReSc*=0.5 at X=20.

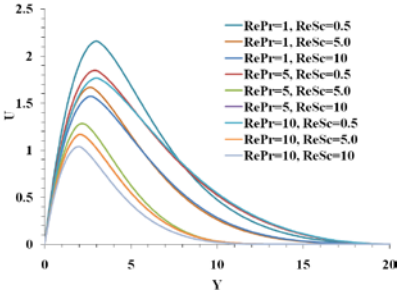

Fig. 3. Steady state velocity profiles for various values of *RePr* and *ReSc* when n=1.5, k_1=0.05, k_2=0.02, *Gr*=*Gm*=0.5 at X=20.

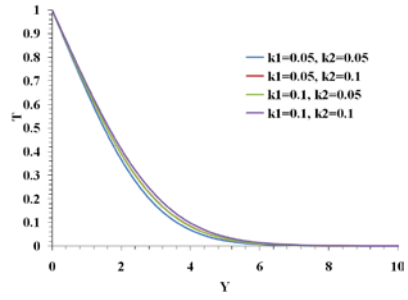

Fig. 4. Steady state temperature for various values of k_1 and k_2 when n=0.5, *Gr*=*Gm*=0.5, *RePr*=5.0 and *ReSc*=0.5 at X=20.

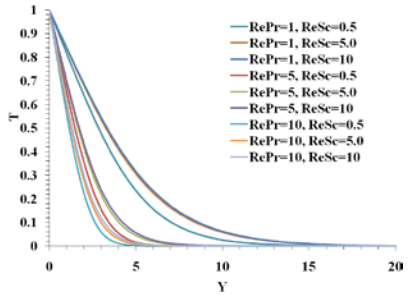

Fig. 5. Steady state temperature for various values of *RePr* and *ReSc* when n=1.5, k_1=0.05, k_2=0.02, *Gr*=*Gm*=0.5 at X=20.

Figs. 2-3 illustrate the velocity function for different values of the parameters t, k_1, k_2, *RePr*, *ReSc*, *Gr* and *Gm*. The effects of k_1 and k_2 on the velocity profiles are shown in Fig. 2. We observe that as the parameters k_1 and k_2 increase, the velocity maximum decreases. It can be seen from Fig. 3 that as the parameters *RePr* and *ReSc* increase,

the velocity maximum decreases. It is interesting to note that the two lines (*RePr*=10, *ReSc*=5) and (*RePr*=5, *ReSc*=10) are coincided when *Gr* equal *Gm*.

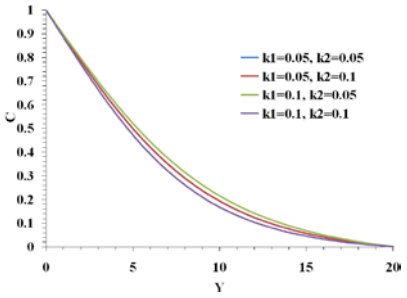

Fig. 6. Steady state concentration for various values of k_1 and k_2 when n=0.5, Gr=Gm=0.5, $RePr$=5.0 and $ReSc$=0.5 at X=20.

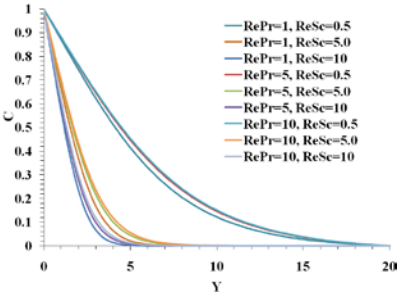

Fig. 7. Steady state concentration for various values of *RePr* and ReSc when n=1.5, k_1=0.05, k_2=0.02, Gr=Gm=0.5 at X=20.

Figs. 4-5 show the temperature profiles for different values of the governing parameters. It is clear from Fig. 4 that as parameters k_1 and k_2 are increasing the temperature profiles are increasing. Also, we observe from Fig. 5 that due to an increase in *RePr* there is reduce in the thermal boundary layer thickness and a fall in the temperature profiles, while, with *ReSc* the opposite is true.

Figs. 6-7 illustrate the concentration distributions for various values of the given parameters. It is clear that as the parameters k_1 and k_2 are increasing the concentration profiles are increasing as shown in Fig. 6. We note from Fig. 7 that due to an increase in *RePr* there is an increase in the concentration profiles, while, with *ReSc* the opposite is true.

References

1. H.T. Chen and C.K. Chen, Trans. ASME, J. Heat Transfer 110 (1998) 257.
2. K.N. Mehta and K.N. Rao, Int. J. Eng. Sc. 32 (1994) 521.
3. A.V. Shenoy, Trans. in Porous Media 11 (1993) 219.
4. A. Nakayama and H. Koyama, Applied Scientific Research 48 (1991) 55.
5. T.R. Roy, Indian J. Pure and Applied Mathematics 10 (1979) 366.
6. S. Haq and J.C. Mulligan, J. Non-Newtonian Fluid Mechanics 36 (1990) 395.
7. F.M. Hady, E.M. Osman and R.A. Mohamed, MMC, B: Solid and Fluid Mech. & Therm. Mech. System 54 (1994) 21.
8. A.A. Raptis, Int. J. Energy Res. 7 (1983) 385.
9. M. Kumari and G. Nath, Int. J. Energy Res. 13 (1989) 379.
10. M. Kumari and G. Nath, Int. J. Energy Res. 13 (1989) 419.
11. M. Kumari and G. Nath, Warme-Stoffubertrag 24 (1989) 103.
12. I. Pop and H. Herwing, Int. Commun. Heat Mass Transfer 17 (1990) 813-821.
13. R. Bradean, D.B. Ingham, P.J. Heggs and I. Pop, Numerical Heat Transfer, Part A 31 (1997) 325.
14. J. Srinivasan and D. Angirasa, Int. J. Heat Mass Transfer 31 (1988) 2033.
15. D. Angirasa, G.P. Peterson and I. Pop, Int. J. Heat Mass Transfer 40 (1997) 2755.
16. S.K. Rastogi and D. Poulikakos, Int. J. Heat Mass Transfer 38 (1995) 935.
17. F.M. Hady and F.S. Ibrahim, Trans. in porous media, 28 (1997) 125.
18. Z.P. Shulman, B.I. Baykov and E.A. Zaltsgendler, Naukai technika, Minsk (in Russian), 1975.
19. Yu. I. Shvets and V.K. Vishevskiy, Heat Transfer-Soviet Research 19 (1987) 38.
20. B. Carnahan, H.A. Luther J.O. Wilkes, Applied numerical methods, John Wiley, New York, 1969.